IntechOpen *Journals*

Digital Medicine and Healthcare Technology

RESEARCH PAPER

T-Cell Receptor Dependent and Independent NF-kappa B Activation is a Prognostic Marker and a Therapeutic Target in Peripheral T-cell Lymphoma Not Otherwise Specified

Mohsen Navari[1,2,3], Maryam Etebari[4], Francesca Ricci[5], Pier Luigi Tazzari[5], Claudio Agostinelli[6], Philip Went[7], Davide Gibellini[8] and Pier Paolo Piccaluga[9,10,11,12,*]

1 Department of Medical Biotechnology, School of Paramedical Sciences, Torbat Heydariyeh University of Medical Sciences, Torbat Heydariyeh, Iran
2 Research Center of Advanced Technologies in Medicine, Torbat Heydariyeh University of Medical Sciences, Torbat Heydariyeh, Iran
3 Bioinformatics Research Group, Mashhad University of Medical Sciences, Mashhad, Iran
4 Department of Medical Genetics, Faculty of Medicine, Mashhad University of Medical Sciences, Mashhad, Iran
5 Service of Transfusion Medicine, IRCCS, S. Orsola-Malpighi Hospital, Bologna, Italy
6 Department of Experimental, Diagnostic, and Specialty Medicine—DIMES, Hematopathology Unit, S. Orsola-Malpighi Hospital, Bologna University School of Medicine, Italy
7 Institute of Pathology, Basel, Switzerland
8 Microbiology Section, Department of Diagnostic and Public Health, Verona University, Italy
9 Department of Experimental, Diagnostic, and Specialty Medicine, Biobank of Research, IRCCS, S. Orsola-Malpighi Hospital, University of Bologna School of Medicine, Bologna, Italy
10 Institute of Hematology and Medical Oncology "L. and A. Seràgnoli", Via Massarenti, 9 - Bologna, Italy
11 Istituto Euro-Mediterraneo di Scienza e Tecnologia (IEMEST) Palermo, Italy
12 Department of Pathology, School of Medicine, Jomo Kenyatta University of Agriculture and Technology, Juja, Kenya
*Corresponding author. Department of Experimental, Diagnostic, and Specialty Medicine, Biobank of Research, IRCCS, S. Orsola-Malpighi Hospital, University of Bologna School of Medicine, Bologna, Italy – Institute of Hematology and Medical Oncology "L. and A. Seràgnoli". Via Massarenti, 9 - 40138 Bologna, Italy. E-mail: pierpaolo.piccaluga@unibo.it

Citation
Mohsen Navari *et al.* (2022), T-Cell Receptor Dependent and Independent NF-kappa B Activation is a Prognostic Marker and a Therapeutic Target in Peripheral T-cell Lymphoma Not Otherwise Specified. *Digital Medicine and Healthcare Technology* 2022(0), 1–28.

DOI
https://doi.org/10.5772/dmht.04

Published
28 March 2022

Abstract

Peripheral T-cell lymphomas not otherwise specified (PTCL/NOS) is the commonest subtype of PTCL. NF–kB related molecules have been found to be variably expressed in PTCL/NOS, suggesting a potential involvement of the NF–kB system in their pathogenesis. However, the actual contribution of NF–kB molecular programs to the PTCL/NOS landscape has not been investigated yet.
In this study, we assessed in a large series of PTCL/NOS, the activation status of NF–kB programs and investigated the prognostic impact of such NF–kB expression. Moreover, we explored the possible role of NF–kB inhibitors. We studied the gene expression profiles of 180 PTCL cases and tested two different drugs, the IKK

inhibitor BMS-345541 and the proteasome inhibitor Bortezomib, in four PTCL cell lines.

We found that most cases (84%) presented with some degree of NF–kB activation, based on the expression of *REL* and *RELA*. Functionally, the latter was strictly related with TCR signaling activation, while REL was at least partially TCR independent. We also identified genes related with NF–kB activation in this setting that were mainly involved in cell proliferation and apoptosis inhibition. Further, by reverse engineering we defined the transcriptional network of both REL and RELA in PTCLs that only partially overlapped. On the clinical ground, we found that RELA expression was related to a significantly poorer overall survival, with similar trends for REL. However, most remarkably, when all the three genes were considered together, cases with at least one gene over-expressed, showed a dramatically inferior overall survival (28.67 vs. 56.018 months; $p = 0.004$). Finally, we showed that NF–kB pharmacological inhibition was associated with cell cycle arrest and cell death in NF–kB positive PTCL cells.

In conclusion, we extensively explored NF–kB activation in PTCL/NOS, documenting its negative prognostic role. Further, we showed that NF–kB inhibition might represent a rational therapeutic approach in selected cases.

Keywords: peripheral T-cell lymphoma, NF kappa B, microarray, immunohistochemistry, targeted therapy, bortezomib

1. Introduction

Peripheral T-cell lymphomas not otherwise specified (PTCL/NOS) is the commonest subtype of PTCL [1, 2]. This is a complex entity, characterized by significant morphologic, immunophenotypic and clinical variability, whose molecular pathology is still largely unknown [3, 4].

Recently, gene expression profiling (GEP) allowed the identification of PTCL/NOS-associated signatures, leading to the better understanding of its histogenesis, pathogenesis and prognostication [5–12]. Interestingly, GEP studies suggested that PTCL/NOS may present with up- or down-regulation of nuclear factor kappa B (NF–kB) molecules [5–7], with possible prognostic relevance [7, 13]. However, these studies investigated a limited number of PTCLs/NOS cases [7, 13] and mostly included cases with prominent non-neoplastic components [6]. In addition, only one NF–kB effector, RelA, has been studied at protein level. By contrast, the NF–kB pathway is a complex system including five main characters (namely, RELA/p65, RELB, REL, p50 and p52 encoded by *RELA, RELB, REL, NFKB1, NFKB2,* respectively) physiologically regulating inflammation, immune response, and cell cycle. When altered, it can be involved in tumorigenesis, and, possibly, in the pathogenesis of human lymphomas, including both B-cell [14] and T-cell derived

ones, such as mycosis fungoides [15], and T-ALL [16]. In this regard, our group showed that a small proportion of PTCLs/NOS presented with *REL* locus genomic abnormalities eventually leading to REL protein nuclear re-localization [17].

Importantly, NF–kB molecules are basically retained in the cytoplasm in an inactive form by specific inhibitors (IKB family members), while exerting their transcription factor activity when located in nuclei upon specific stimulation. To be functional, NF–kB effectors need to constitute specific dimers which activate the so called canonical (RELA/p50, RELA/RELA, p50/REL and RELA/REL) and alternative (RELB/p52) pathways. The transcription activation domain (TAD) necessary for the positive regulation of gene expression is present only in RELA/p65, REL and RELB [18]. By contrast, as they lack TADs, p50 or p52 may repress transcription unless associated with TAD-containing NF–kB family member [18].

In T-lymphocytes, NF–kB activation is mainly induced by the T-cell receptor (TCR) signaling, that is commonly abrogated in some PTCL such as anaplastic large cell lymphoma [19] and, possibly, in a fraction of PTCL/NOS [20] and angioimmunoblastic lymphomas (AITL) [21].

As NF–kB is a suitable therapeutic target in cancer, bortezomib, a selective inhibitor of the proteasome 26S, involved in the NF–kB cell signaling regulation, has been evaluated for treatment of patients with PTCL. A Phase I study of bortezomib used in association with CHOP chemotherapy was conducted in 13 patients with advanced PTCL or NK/T-cell lymphoma [22]. The reported CR rate was 62%, with no data published on PFS or OS. A phase II study of bortezomib as a single agent for patients with relapsed PTCL (n = 2) or cutaneous T-cell lymphoma (CTCL) (n = 13) reported objective response rates (ORR) of 67%, with a duration of response ranging from 7 to 14 months and both patients with PTCL achieving CR [23]. Recently, results of a Phase II trial combining bortezomib to CHOP chemotherapy in the frontline setting for patients with stage III/IV PTCL were published [24]. Of the 46 patients enrolled, 30 achieved a CR (65%), with an ORR of 76%. Despite good initial response rates, the 3-year OS and PFS rates were 47 and 35% respectively, indicating that a fraction of patients does not benefit from the addiction of a NF–kB inhibitor.

In this study, we assessed in a large series of PTCL/NOS, the activation status of Nf-kB programs by focusing for the first time on all the main components, representing both the canonical and alternative pathways, and investigated the relation with TCR signaling as well as the prognostic impact of such NF–kB expression. Moreover, we explored the possible role of NF–kB inhibitors in this setting.

2. Materials and methods

2.1. Gene expression analysis

We studied 180 PTCLs from which GEP were previously generated using fresh/frozen tissues [9–11, 21] (GEO data sets: GSE6338 and GSE19069). All of the cases were reviewed by at least two expert hematopathologists and diagnosed according to the WHO Classification [2]; furthermore, the diagnosis was refined by applying a molecular classifier recently developed by our group [10]. The detailed clinicopathological characteristics of these cases were previously reported [10].

Specifically, to characterize the activation of NF–kB pathway, we studied the expression of RELA (201783_s_at and 209878_s_at), RELB (205205_at), and REL (206035_at, and 206036_s_at), as well as the one of a series of well-known NF–kB targets, previously used for analogue purposes [14] and validated biochemically (http://www.bu.edu/nf-kb/gene-resources/target-genes/; http://bioinfo.lifl.fr/NF-KB/) [25]. Further, we studied genes encoding for proteins involved in TCR signaling [19].

Raw data were normalized in GeneSpring GX 12.5 (Agilent, CA); details on sample normalization and analysis have been previously reported [9–11, 21, 26, 27]. Reverse engineering was carried on by ARACNe algorithm in GeWorkbench 2.6.0 as previously described [27, 28]. Possible relationships among genes were further investigated by Cognoscente (http://vanburenlab.tamhsc.edu/cognoscente).

Gene expression studies were conducted according to MIAME guidelines. Raw gene expression are available at http://www.ncbi.nlm.nih.gov/projects/geo/.

2.2. Cells culture

Four human PTCL cell lines (Fe–Pd, Mac1, Karpass-299, and Jurkat) served as in vitro PTCLs models for treatment with BMS-345541 (SigmaAldrich) and Bortezomib (kindly provided by Dr. Guarguaglini). BMS-345541 (4(2′-aminoethyl) amino-1,8-dimethylimidazo (1,2-α)-quinoxaline)-4,5-dihydro-1,8-dimethyli-midazo (1,2-α)quinoxalin-4-one-2-carboxylic acid, was dissolved in DMSO to produce a 10 mM (mmol/L) stock solution while, Bortezomib was dissolved in water at 1 mM stock solution concentration. The FE-PD cell line was kindly provided by Annarosa del Mistro (Padova University, Italy). The NPM-ALK + ALCL Karpas 299 and CTLC MAC1 were kindly provided by Prof. Inghirami (Department of Pathology and CERMS, University of Torino, Turin, Italy). Jurkat cell line (T-ALL) was purchased from DSMZ cell collection (Braunschweig, Germany). In this study Jurkat cell line was considered as negative control of BMS-345541 treatment as already reported in other study [29]. We also analyzed Pheripheral blood mononuclear cells (PBMC)

obtained from healthy donor. Briefly, PBMC were separated by ficoll gradient density centrifugation using Lympholyte-H (Cedarlane Laboratories).

All the four cell lines and PBMC were cultured in RPMI medium 1640 containing 10% FBS and 2 mM L-glutamine (Lonza).

2.3. Cell viability assessment

Cell viability was measured by CellTiter-Glo Luminescent Cell Viability Assay (Promega,Corporation Italy). Aliquots of 5×10^4 cells per well were distributed in 96-well opaque microplates in 100 μl of medium and incubated at 37 °C in a 5% CO_2 humidified incubator for 48 h. BMS-345541 and Bortezomib were added at progressively increasing concentrations ranging from 0.1 μM up to 9 μM and from 2 nM up to 15 nM, respectively, to determine growth inhibition curves for all cell lines. Following incubation, 100 μl of CellTiter-Glo Reagent was added to the volume of cell culture medium present in each well, according to the manufacturer's instructions. The relative cell viability was determined at 490 nm using a Victor2 (PerkinElmer) 96-well plate reader instrument. Each experiment was performed in triplicate.

For each cell line the value of half maximal inhibitory concentration (IC_{50}) [30, 31] was computed using the GraphPad software.

2.4. Flow-cytometry

To evaluate apoptosis and cell cycle, the four cell lines were incubated for 48 h with and without BMS-345541 (3.5, 4, 5 and 6 μM) and Bortezomib (5 and 8 nM).

In order to detect and quantify apoptosis we used Annexin-V-Fluos staining kit (Roche, Italy). Cells were harvested, washed twice and re-suspended in 100 μl of Annexin-V-Fluos labeling solution for 15 min, according to the manufacturer's instructions. Then, we added 500 μl of incubation Buffer and analyzed with NAVIOS cytometer (Beckman Coulter). Data were elaborated by Kaluza dedicated software. Annexin V + PI-cells represented the early apoptotic populations. Annexin V + PI + cells represented either late apoptotic or secondary necrotic populations.

We followed the progression of S-phase through the cell cycle by labeling cells with the thymidine analog 5-bromo-2′-deoxyuridine (BrdU) (Roche). After treatments, cells were collected and fixed to analyze the embedding of Br-dU according to the manufacturer's instructions. The progression of labeled cells through the cell cycle was quantified by measurement of the fraction of BrdU-labeled cells in S-phase,G2/M, and G1 by flow-cytometry NAVIOS cytometer (Beckman Coulter).

Table 1. Immunohistochemical expression of RELA, REL, and p(Ser 727)-STAT3.

Molecule	Source	Dilution	Retrieval	Revelation system
REL	Santa Cruz Inc.	1:20	PtLink, high pH 92 °C × 20 min	K8012*
RELA	Santa Cruz Inc.	1:20	PtLink, high pH 92 °C × 20 min	K8012*
p(Ser 727)-STAT3	Cell signaling technology	1:25	PtLink, high pH 92 °C × 20 min	K8012*

*K5005: Real detection system alkaline phosphatase/RED rabbit/mouse (Dako Cytomation, Denmark).

2.5. Cytochemistry

To assess the effective inhibition of Nf-kB pathway via IKK inhibitor, we used immunohistochemistry by staining the Fe–Pd cell line after 6 h of treatment with 5 μM of BMS-345541. Briefly, cells were collected, washed once with cold phosphate-buffered saline (PBS), and centrifuged at 1500 r.p.m. for 5 min. The cell pellets were fixed in PBS-buffered formalin at room temperature at least 2 h. The cells were centrifuged for 10 min, then the cell pellets were washed with physiological saline and centrifuged. Subsequently, we added to the cell pellets human plasma and Simplastin (Tromborel) in ratio of 1:2 to allow formation of the clot. Finally, the clots were then routinely embedded in paraffin wax, as described previously [32], and processed for the detection of RELA and P50 by IHC. Briefly, FFPE clots were investigated by antibodies raised against fixation resistant epitopes: RELA (mouse monoclonal; Santa Cruz Inc.) and p50 (rabbit polyclonal; Thermo Scientific). The antigen retrieval protocols, dilutions and revelation system are detailed in table 1. Immunohistochemical preparations were visualized and images were captured using Olympus Dot-slide microscope digital system equipped with the VS110 image analysis software.

2.5.1. Immunohistochemistry

NF–kB pathway activation status was also evaluated on formalin-fixed paraffin-embedded (FFPE) samples corresponding to 48 PTCL/NOS. All the cases were retrieved from the archives of the Haematopathology Unit, Department of Experimental, Diagnostic and Specialty Medicine—DIMES, University of Bologna. The study was conducted according to the principles of the Helsinki declaration after approval of the Internal review Board. Two different tissue-microarrays (TMAs) were constructed from these paraffin-embedded blocks as previously reported [33]. TMAs sections were investigated by antibodies raised against fixation resistant epitopes; REL (rabbit polyclonal; Santa Cruz Inc.), RELA (mouse monoclonal; Santa Cruz Inc.), and p(Ser 727)-STAT3 (1:25) (Cell Signaling Technology, Beverly, MA).

The antigen retrieval protocols, dilutions and revelation system are detailed in table 1. Notably, each TMA was also tested with anti-CD20 and CD3 antibodies to define the number of reactive B-cells comprised within the neoplastic T-cell population. Each section was independently evaluated by at least two experienced hematopathologists. NF–kB pathway in each case was scored as activated if more than 30% of the examined neoplastic cells showed nuclear positivity for one or more among transcription factors REL, RELA (canonical pathway) Immunohistochemical preparations were visualized, and images were captured using Olympus Dot-slide microscope digital system equipped with the VS110 image analysis software.

Each section was independently evaluated by at least two experienced hematopathologists. Cases were considered positive if 30% or more of the tumor cells were stained with antibody. The number of positive cells was estimated by each observer. The intensity of staining was also evaluated, but not used to determine positivity, as it can vary with the degree of tissue fixation. All the 48 cases included in the TMA had also been studied by GEP.

2.6. Statistical analysis

Statistical analyses were carried on with the IBM SPSS Statistics 20.0 (IBM, USA). Anova, and unpaired T-Test were adopted for GEP data analyses. Survival data were analyzed by using the Kaplan-Meier method [34]. Specifically, overall survival (OS) was calculated from the time of diagnosis to death or last follow up; progression free survival (PFS) was calculated from the end of induction treatment until progression, death, or last contact. Clinical information and complete follow up were available for 43/48 cases.

The limit of significance for all analyses was defined as $P < 0.05$; two-sided tests were used in all calculations.

All cases were collected at diagnosis, before any treatment administration. The study was approved by the Local Ethical Committee and conduced according to the Helsinki Declaration principles.

3. Results

3.1. NF–kB REL components are variably expressed in PTCL

First, we studied the expression of *RELA*, *RELB* and *REL* in a series of 180 PTCL cases. We documented variable expression levels across the panel (figure 1A). As high levels of NF–kB effectors (*RELA*, *RELB*, and *REL*) have been previously related to NF–kB pathway activation, we divided our series into quartiles (Q1-4), based on the expression of each molecule (figure 1A). We then used GSEA to assess which

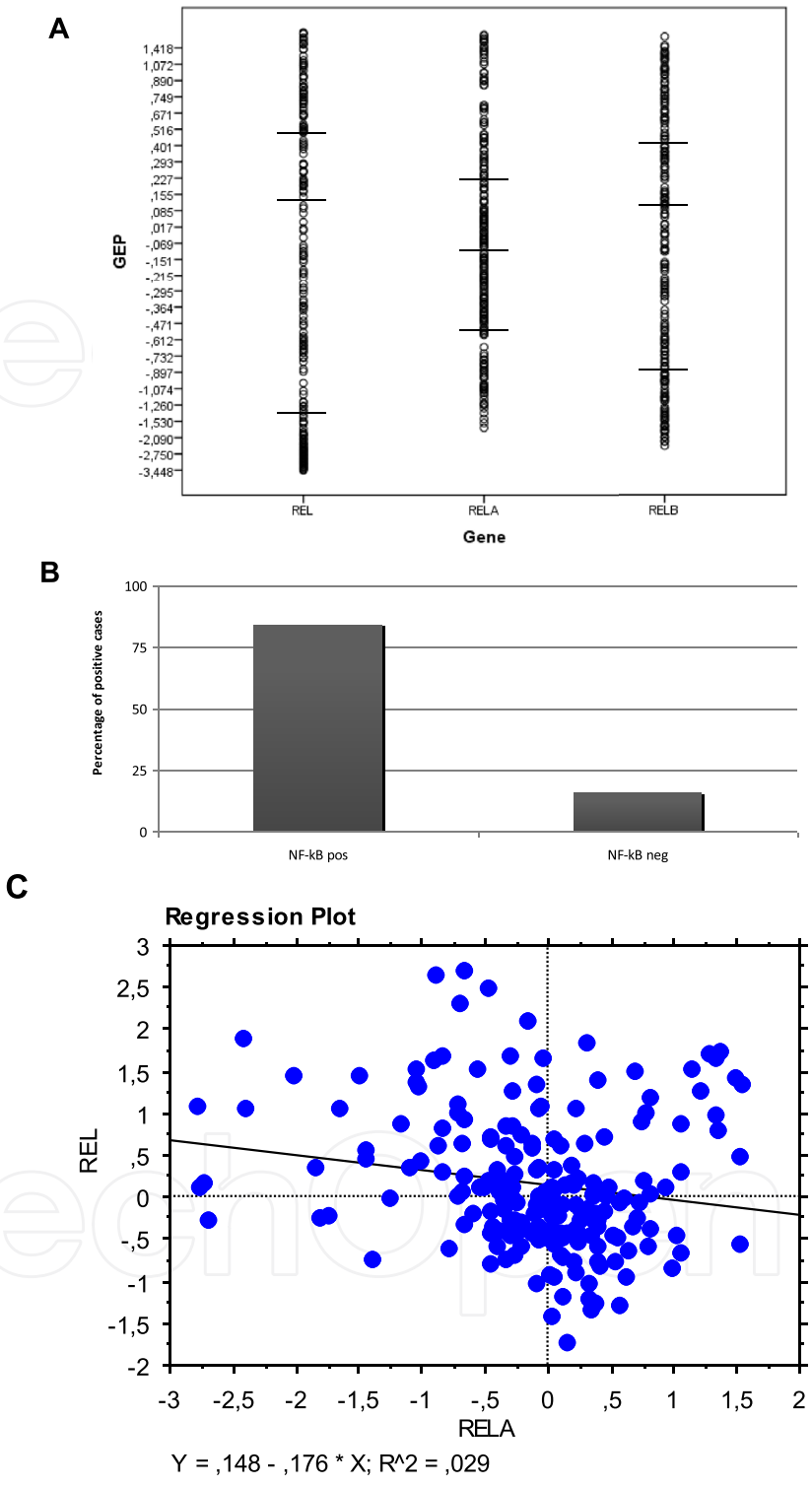

Figure 1. Gene expression of REL, RELA, and RELB in PTCLs. Normalized gene expression values are plotted. Bars delimitate quartiles defined based on gene expression for each one of the three molecules (A). Cases with at least one of the three molecules (*REL*, *RELA*, and *RELB*) in Q2, Q3 or Q4 were classified as NF–kB positive. Cases with all RELs in Q1 were classified as NF–kB negative (B). Notably, RELA and REL expression appeared to be inversely related (C).

group(s) could present with functional signs of NF–kB activation. Interestingly, we found a significant enrichment in both NF–kB targets and NF–kB pathway (as defined by GeneOntology) in Q2, Q3, and Q4 for *RELA* and *REL*. Conversely, no enrichment was recorded for any *RELB* subgroup. Therefore, we classified samples as NF–kB positive (84%) if falling in Q2-4 for at least one out of *RELA* and *REL*, and NF–kB negative (16%) in any other circumstance (figure 1B). Interestingly, *REL* and *RELA* expression tended to be mutually exclusive as documented by the inverse relation ($r2 = 0.29$; $p = 0.01$; figure 1C), though cases with high or null expression of both were recorded.

To further test whether such division could be reliable, we performed a supervised analysis between the two groups (NF–kB positive vs. NF–kB negative) and identified 781 probe sets, corresponding to 668 unique genes, that were differentially expressed in the two groups (figure 2A; supplementary table 1). Based on the expression of these genes, cases were then clustered and roughly separated according to NF–kB activation (figure 2B). Of interest, when we sought for pathways and cellular programs enriched in these genes, we found, among others, the TCR signaling (the main upstream of NF–kB in T-cells), the NF–kB pathway cascade itself, and the NF–kB transcriptional targets (figure 3; supplementary tables 2–4).

Noteworthy, IHC did confirm GEP data, with nuclear RELA/REL expression in activated cases (figure 4). Specifically, 17/17 NF–kB positive cases showed nuclear staining for either RELA or RELB or REL. Conversely, none of the 24 negative cases presented nuclear staining of a REL family component (table 2).

Together, these data indicated that PTCL/NOS category includes two discrete subgroups apparently characterized by activated and non-activated NF–kB pathway. As RELA and REL but not RELB were involved, it appeared that the canonical rather than the alternative pathway was activated in PTCL/NOS.

3.2. RELA/NF–kB activation is related to TCR signaling activation in PTCL/NOS

As NF–kB pathway is a downstream of TCR signaling in T-lymphocytes, we then focused on the expression of genes representative of TCR signaling (Unigene) [19]. We found several genes differentially expressed between cases with or without NF–kB activation, including *FAS* ($p = 0.007$), *CFLAR* ($p < 0.001$), *CASP1* ($p < 0.001$), *LCK* ($p < 0.001$), *FOS* ($p = 0.01$), *NFKB1* ($p < 0.001$), *NFKBIA* ($p = 0.01$), and *MAP2K4* ($p = 0.002$), *PIK3CG* ($p < 0.001$), *LAT* ($p < 0.001$), *PRKCB* ($p < 0.001$), and *ZAP70* ($p < 0.001$). Consistently, the two groups were clearly discriminated when clustered based on the expression of the TCR-related signature (figure 5; supplementary table 5). Moreover, among genes differentially expressed based on NF–kB activation status, we found genes encoding for TCR components (*CD3E*,

Table 2. Immunohistochemical expression of NF–kB components in PTCLs/NOS.

Case #	RELA result	RELA localization	RELB result	RELB localization	REL result	REL localization	NF–kB at GEP
PTCL NOS 1	Positive	C	Positive	C	Positive	C	Negative
PTCL NOS 2	Positive	C	Positive	C	Positive	C	Negative
PTCL NOS 3	Positive	C	Positive	C	Positive	C	Negative
PTCL NOS 4	Positive	C	Positive	C	Positive	C	Negative
PTCL NOS 5	Positive	C	Positive	C	Positive	C	Negative
PTCL NOS 6	Positive	C	Positive	C	Positive	C	Negative
PTCL NOS 7	Positive	C	Positive	C	Positive	C	Negative
PTCL NOS 8	Positive	C	Positive	C	Positive	C	Negative
PTCL NOS 9	Positive	C	Positive	C	Positive	C	Negative
PTCL NOS 10	Positive	C	Positive	C	Positive	C	Negative
PTCL NOS 11	Positive	C	Positive	C	Positive	C	Negative
PTCL NOS 12	Positive	C	Positive	C	Positive	C	Negative
PTCL NOS 13	Positive	C	Positive	C	Positive	C	Negative
PTCL NOS 14	Positive	C	Positive	C	Positive	C	Negative
PTCL NOS 15	Positive	C	Positive	C	Positive	C	Negative
PTCL NOS 16	Positive	C	Positive	C	Positive	C	Negative
PTCL NOS 17	Positive	C	Positive	C	Positive	C	Negative
PTCL NOS 18	Positive	C	Positive	C	Positive	C	Negative
PTCL NOS 19	Positive	C	Positive	C	Positive	C	Negative
PTCL NOS 20	Positive	C	Positive	C	Positive	C	Negative
PTCL NOS 21	Positive	C	Positive	C	Positive	C	Negative

Table 2. (Continued)

Case #	RELA result	RELA localization	RELB result	RELB localization	REL result	REL localization	NF–kB at GEP
PTCL NOS 22	Positive	C	Positive	C	Positive	C	Negative
PTCL NOS 23	Positive	C	Negative	NA	Positive	C	Negative
PTCL NOS 24	Positive	C	Negative	NA	Positive	C	Negative
PTCL NOS 25	Positive	NC	Positive	C	Positive	C	Positive
PTCL NOS 26	Positive	NC	Positive	C	Positive	C	Positive
PTCL NOS 27	Positive	NC	Positive	C	Positive	C	Positive
PTCL NOS 28	Positive	C	Positive	C	Positive	NC	Positive
PTCL NOS 29	Positive	C	Positive	C	Positive	NC	Positive
PTCL NOS 30	Positive	C	Positive	C	Positive	NC	Positive
PTCL NOS 31	Positive	C	Positive	C	Positive	NC	Positive
PTCL NOS 32	Positive	C	Positive	C	Positive	NC	Positive
PTCL NOS 33	Positive	C	Positive	C	Positive	NC	Positive
PTCL NOS 34	Positive	C	Positive	C	Positive	NC	Positive
PTCL NOS 35	Positive	C	Positive	C	Positive	NC	Positive
PTCL NOS 36	Positive	NC	Positive	C	Positive	NC	Positive
PTCL NOS 37	Positive	NC	Positive	C	Positive	NC	Positive
PTCL NOS 38	Positive	NC	Positive	C	Positive	NC	Positive
PTCL NOS 39	Positive	C	Positive	NC	Positive	C	Positive
PTCL NOS 40	Positive	C	Positive	NC	Positive	C	Positive
PTCL NOS 41	Positive	C	Negative	NA	Positive	NC	Positive

C = cytoplasmic. N = nuclear. NA = not available. Localization = nuclear vs cytoplasmic staining. GEP = gene expression analysis.

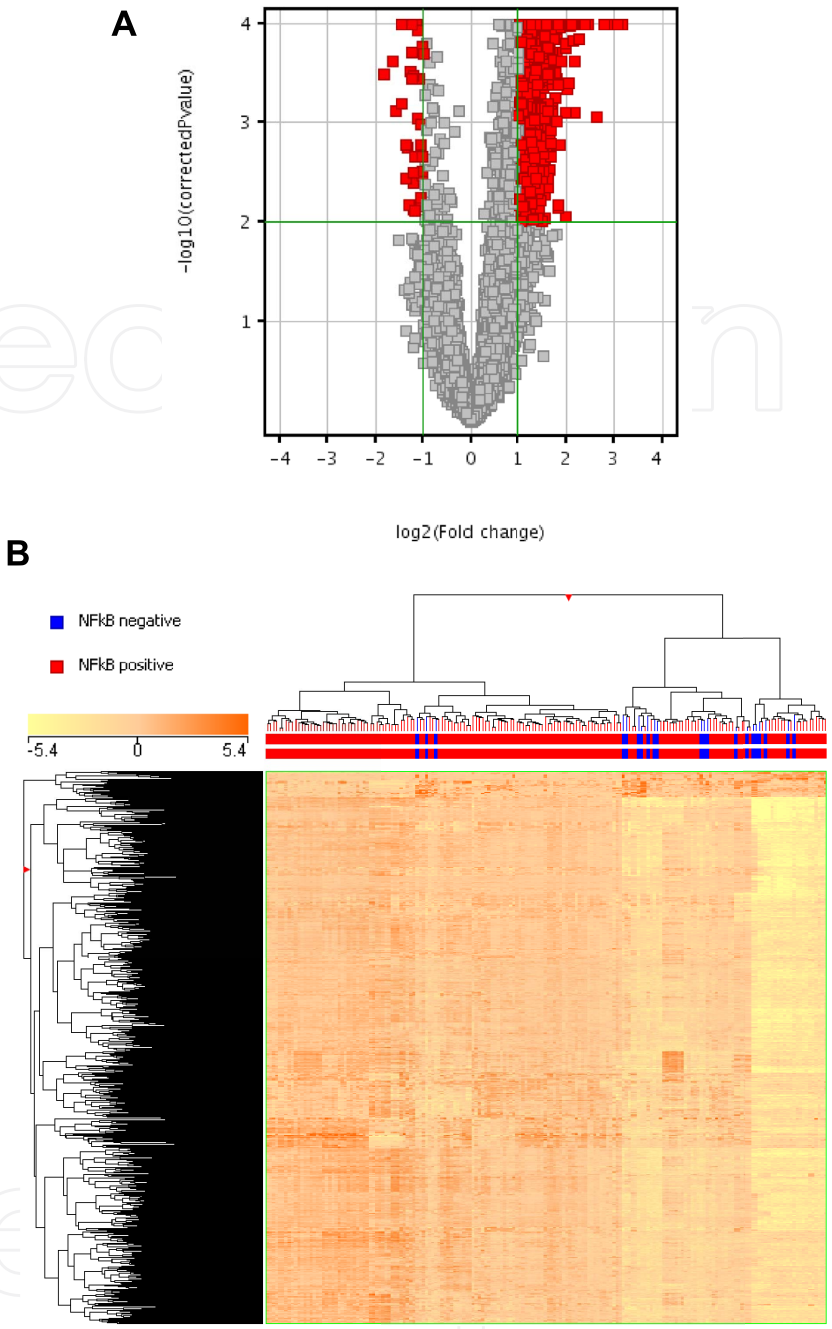

Figure 2. Supervised analysis based on NF–kB molecules expression. Volcano plot showing differentially expressed genes based on p value <0.05 and fold change ≥2 in NF–kB positive vs. NF–kB negative cases (A). Based on the expression of such genes (corresponding to 781 probe sets) cases were clustered (B). The dendrograms are generated using a hierarchical clustering algorithm based on the average-linkage method. In the matrix, each column represents a sample and each row represents a gene. The colour scale bar shows the relative gene expression changes normalized by the standard deviation (0 is the mean expression level of a given gene).

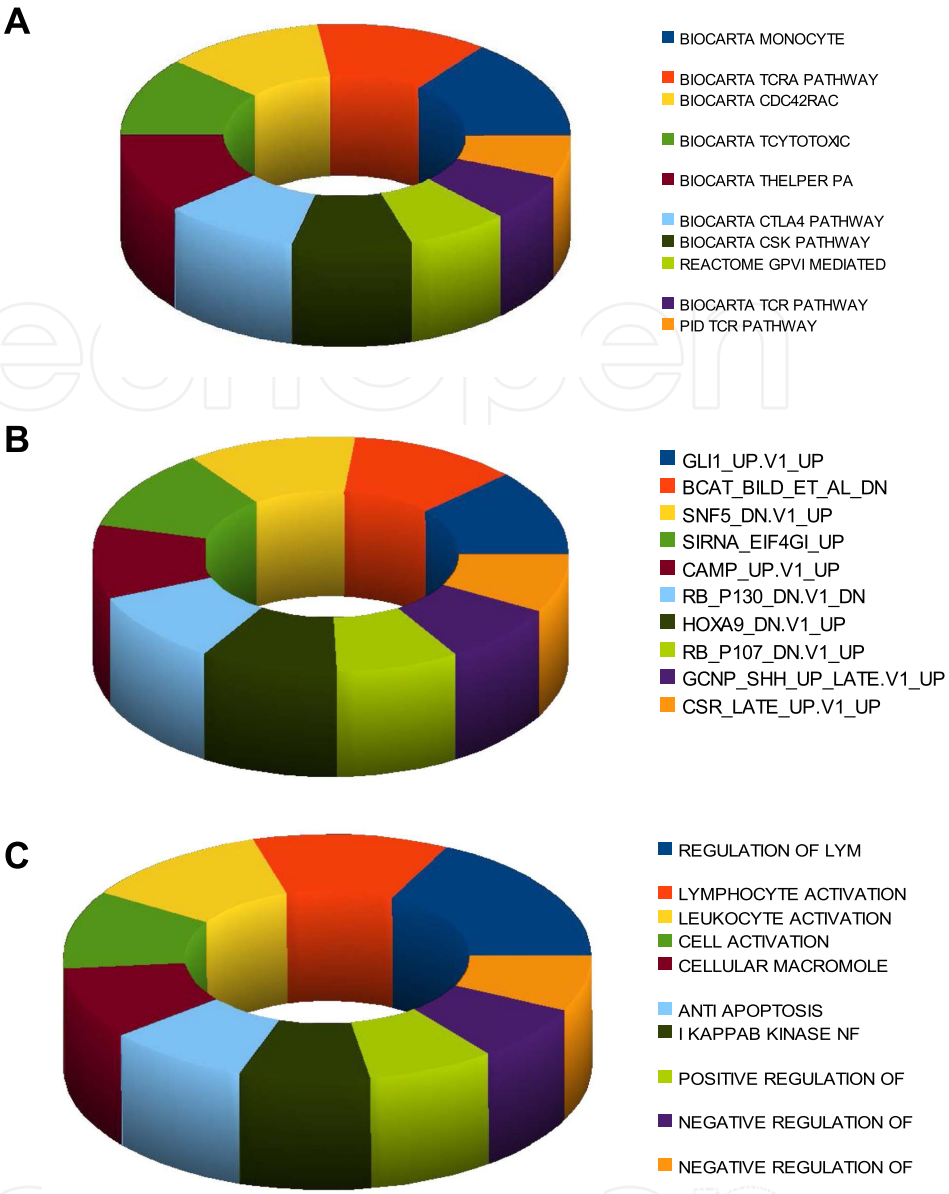

Figure 3. GSEA. Gene set enrichment analysis for genes differentially expressed in NF–kB positive vs. NF–kB negative cases concerning Curated Pathways (A), Oncogenic pathways (B), and GeneOntology Biological Processes (C).

CD5, and *CD7*) as well as TCR costimulatory molecules (*CTLA4*, *CD28* and *ICOS*) (supplementary figure 1).

We then investigated whether *RELA* and *REL* were related to TCR at the same extent. We found that *RELA* expression was directly correlated to that one of both *CD3E* and *CD7* ($p < 0.0001$ and $p < 0.0001$, respectively; supplementary figure 2A–B). Conversely, we observed that *REL* presented an inverse correlation

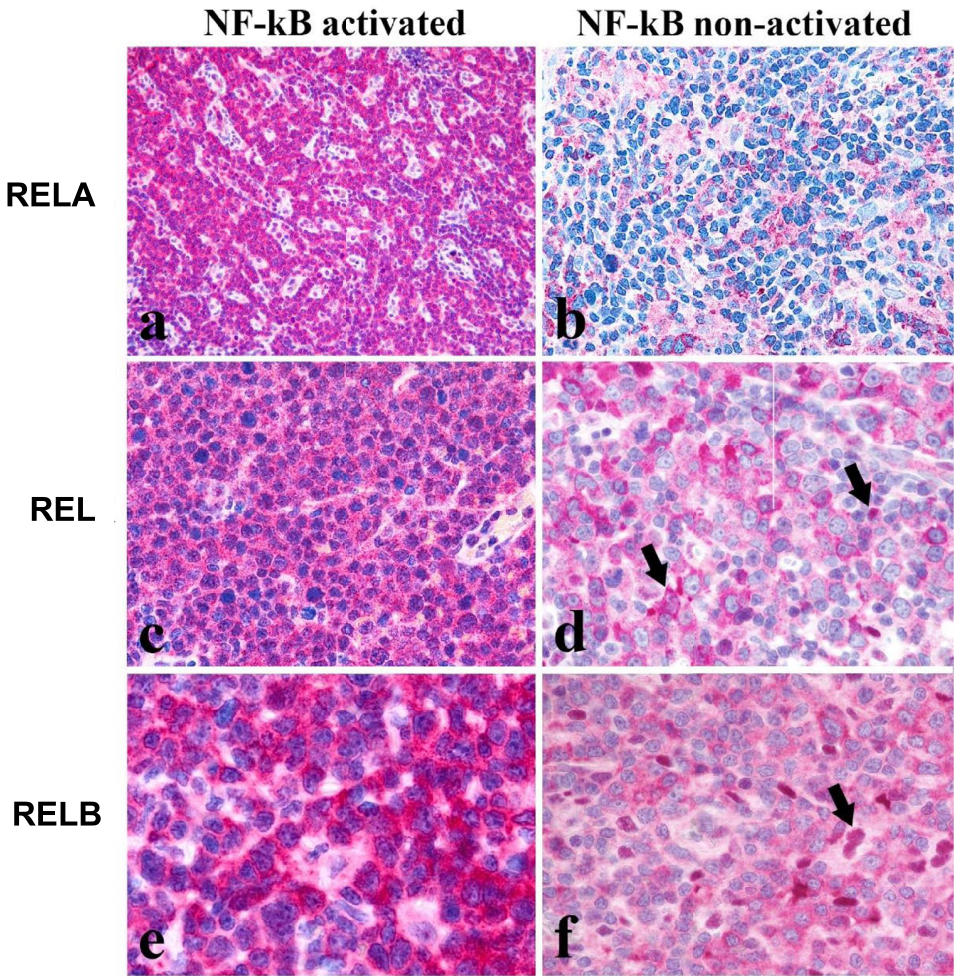

Figure 4. NF–kB activation at protein level. Immunohistochemistry confirmed RELA, RELB, or REL nuclear expression in cases classified as NK-kB positive by GEP. In negative cases, internal controls excluded technical pitfalls (arrows).

with *CD3E* and *CD7* ($p < 0.0001$ and $p = 0.0015$, respectively; supplementary figure 2C–D). In line with this evidence, *RELA* expression was directly correlated with the expression of the downstream molecules *STAT1* and *STAT3* (supplementary figure 2E–F), while *REL* presented an inverse relation with both (supplementary figure 2G–H).

When the costimulatory molecules were considered, *RELA* expression turned out to be directly correlated with that of *CTLA4*, *CD28* and *ICOS,* while *REL* presented with no significant relations (supplementary figure 3).

Together, these data indicate that NF–kB activation is mediated by TCR signaling and RELA in a fraction of PTCL/NOS cases, being at least partially TCR independent and REL associated in other instances.

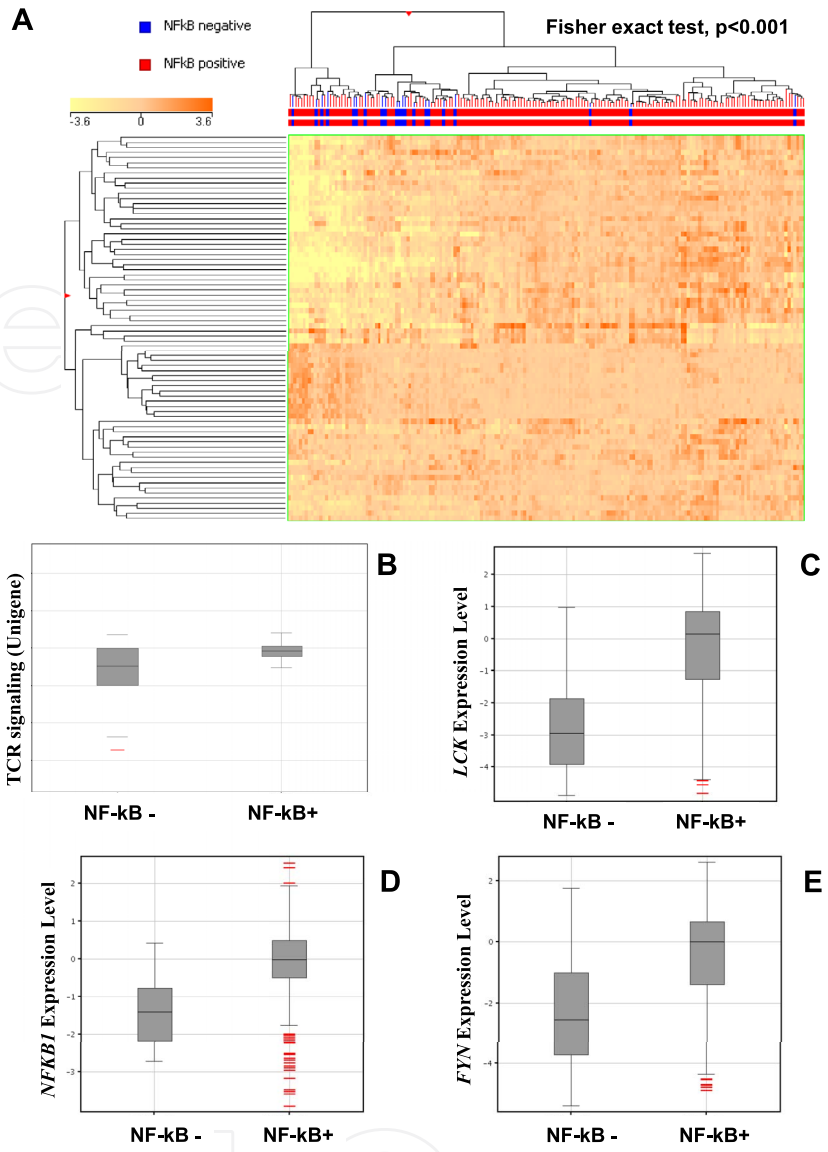

Figure 5. TCR signaling genes in NF–kB positive vs. NF–kB negative PTCLs. PTCLs clustering based on the expression of genes belonging to TCR signaling (A). The dendrograms are generated using a hierarchical clustering algorithm based on the average-linkage method. In the matrix, each column represents a sample, and each row represents a gene. The colour scale bar shows the relative gene expression changes normalized by the standard deviation (o is the mean expression level of a given gene). Average expression values of TCR signalling genes in NF–kB positive vs. NF–kB negative PTCLs (B); *LCK* (C), *NFKB1* (D), and *FYN* (E) expression levels in NF–kB positive vs. NF–kB negative PTCLs. The latter three were chosen as examples among genes differentially expressed in the two groups and belonging to the TCR signaling.

3.3. Reverse engineering revealed similarities and differences between RELA and REL transcriptional networks

As RELA and REL appeared to be activated at least in part by different mechanisms (i.e. TCR dependent or independent), we used reverse engineering to characterize their functional networks aiming to identify possible similarities and differences. To do this, we applied ARACNe, an algorithm previously found to be very effective in recognizing transcription factors targets as well as other molecules functionally related to them. We identified 281 genes significantly related to REL and 849 genes significantly related to RELA. Within the two networks, 133 and 723 genes were univocally related to *REL* or *RELA*, respectively. By contrast, of note, 161 genes were in common, the overlap thus being highly significant ($p < 0.0001$; figure 6A; supplementary figure 4; supplementary table 6). Such 161 genes, when tested for possible functional connection were found to have 147 already proved interactions (supplementary table 7; figure 6B). Among others, we identified *CD44*, *IER2*, *NR3C1*, and *PGK1* as known NF–kB targets as well as *ARID1A*, *BRK1*, *BTG1*, *CCNL1*, *CXCR4*, *FYN*, and *RHOA* all previously related to neoplastic phenotype in humans.

The value of the identified networks was then further validated demonstrating by GSEA their significant enrichment in genes already found to be *REL/RELA* transcriptional targets (obtained from http://www.bu.edu/nf-kb/gene-resources/target-genes/ and http://bioinfo.lifl.fr/NF-KB/) ($p = 0.004$ and $p = 0.005$ for *RELA* and *REL*, respectively). In addition, they largely corresponded to the gens found to be differentially expressed in NF–kB positive vs. NF–kB negative cases ($p < 0.0001$).

Together, these data documented that RELA and REL are involved in partially different functional networks in PTCLs, but do also share a significant number of first neighbor

3.4. NF–kB activation is associated with adverse outcomes in PTCL/NOS

As PTCL/NOS appeared to be composed by two populations according to NF-KB molecular pathway, we sought to investigate the possible prognostic significance of such distinction.

When we studied the overall survival of patients divided in the 4 quartiles, we observed that patients with lower levels of *RELA* and *REL* fared better (figure 7). Similarly, when cases were divided into two groups based on *REL* and *RELA* expression (positive vs. negative; positive being defined when at least one gene was highly expressed), we observed a clear–cut differences between cases with higher or lower *RELA* and *REL* levels (figure 7). Particularly, the difference appeared to be significant as far as *RELA* was concerned. Most interestingly, when cases were

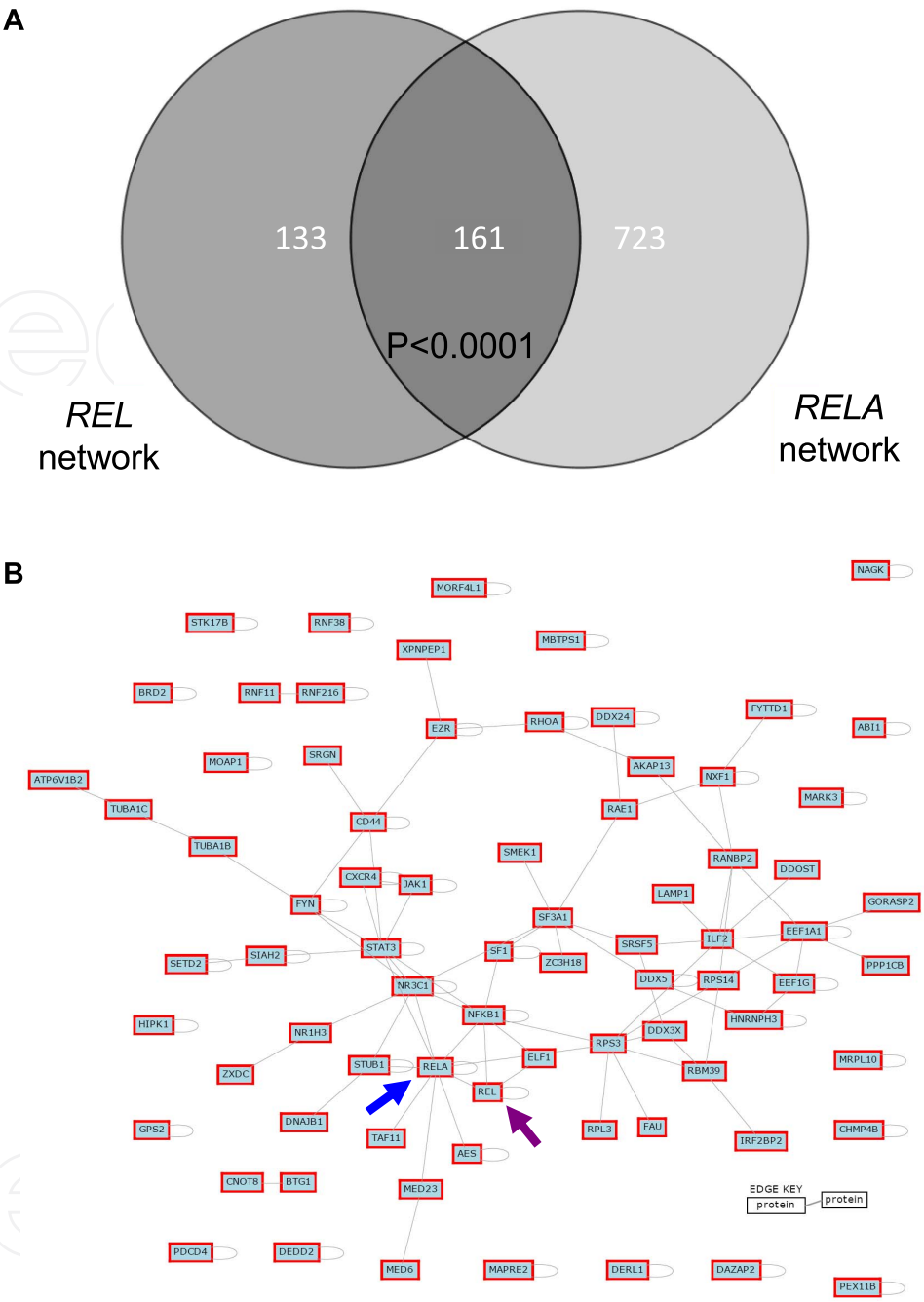

Figure 6. Interaction network of RELA and REL targets evaluated by Cognoscente software. (A) Venn diagram showing common targets between the two networks. (B) Actual networks of the two transcription factors.

grouped as NF–kB positive vs. NF–kB negative, by considering *REL* and *RELA* together, we documented a significantly different OS. Specifically, the estimated mean OS for NF–kB positive cases was 28.67 (95% CI, 15.875–41.459) vs. 56.018

months (95% CI, 39.252–72.785) (p = 0.004; figure 7). By contrast, in line with its inactivity indicated by GEP, *RELB* expression was not associated with the clinical outcome. Survival data are summarized in table 3.

3.5. Canonical NF–kB pathway is activated in PTCL cell lines

We established whether NF–kB pathway was active in the four available cell lines. Based on GEP, Fe–Pd, Mac1, Karpass-299, and Jurkat cells were considered RELA-positive, REL-positive, and RELB-negative. Consistently, RELA (p65), REL and p50, representative of the canonical pathway, showed a nucleus-cytoplasmic localization at immunofluorescence, while RELB and p52 typical of the alternative pathway, appeared to be confined to the cytoplasm, indicating an active and inactive status for the canonical and alternative pathways, respectively (supplementary figure 5).

3.6. NF–kB inhibition through BMS-345541 and Bortezomib limits proliferation and induces apoptotic cell death in PTCL cell lines

We then sought to assess whether NF–kB pathway shut off could affect the cellular vitality of PTCL cells. We used BMS-345541, a specific IKK inhibitor (upstream NF–kB activator) as well as Bortezomib, a proteasome inhibitor. The latter, though less specific, is already available in the clinical practice and determines NF–kB blockage via proteasome inhibition [35].

To verify whether BMS-345541 and Bortezomib could inhibit PTCL cell growth we used increasing concentrations of the two drugs from 0.1 μM to 9 μM and 2 nM to 15 nM for 48 h, respectively. The cell growth of PTCL cells was inhibited in a dose-dependent manner. Specifically, the IC50 values for BMS-345541 (figure 8A) and Bortezomib (figure 8B) at 48 h for the four cells lines were as follows: Fe–Pd 5 μM and 8 nM; MAC1 6.5 μM and 10 nM; Karpas 6.97 μM and 9.63 nM; Jurkat >12 μM and >15 nM (table 4). Jurkat cells were resistant to BMS-345541 and Bortezomib treatment, as expected.

We then investigated whether NF–kB inactivation could be responsible for PTCL cell cycle progression arrest and induction of cell death. To evaluate the effect of NF–kB inhibition over cell cycle progression we considered 5 μM and 8 nM for BMS-345541 and Bortezomib, respectively, corresponding to their Ic50. After measurement of the fraction of BrdU-labeled cells by flow-cytometry, we observed an arrest of cell cycle in G0/G1 phase in Fe–Pd (68% for BMS-345541 and 73.6% for Bortezomib), Mac1 (33% for BMS-345541 and 47% for Bortezomib), Karpas (50% for BMS-345541 and 48% for Bortezomib). On the contrary, Jurkat cells were insensitive to both the treatments (16% for BMS-345541 and 19% for Bortezomib) (figure 8).

We subsequently evaluated the apoptosis rate by Annexin V assay in PTCL cells lines treated or not with BMS-345541 and Bortezomib as single agents at different

Table 3. OS of PTCL patients according to NF–kB component expression levels.

	Means and medians for survival time								Log rank (Mantel-Cox)
			95% Confidence interval				95% Confidence interval		
	Estimate	Std. error	Lower bound	Upper bound	Estimate	Std. error	Lower bound	Upper bound	
RELA			Mean[a]				Median		0.045
$RELA^{26-100}$	29.881	7.019	16.124	43.639	13.000	2.867	7.381	18.619	
$RELA^{0-25}$	42.020	7.501	27.318	56.721					
Overall	38.713	8.438	22.175	55.251	15.600	2.914	9.888	21.312	
REL			Mean[a]				Median		0.099
REL^{26-100}	30.715	7.363	16.283	45.147	13.043	2.356	8.426	17.660	
REL^{0-25}	38.539	7.457	23.922	53.155	29.766	16.384	0.000	61.879	
Overall	38.713	8.438	22.175	55.251	15.600	2.914	9.888	21.312	
RELB			Mean[a]				Median		0.786
$RELB^{26-100}$	1722.278	408.747	921.134	2523.422	455	260.817	0	966.201307	
$RELB^{0-25}$	1004.100	264.284	486.104	1522.096	377.000	288.108	0.000	941.691	
Overall	1766.654	332.243	1115.457	2417.851	455.000	159.198	142.971	767.029	
RELA+REL			Mean[a]				Median		0.004
NFkB neg	56.018	8.554	39.252	72.785					
NFkB pos	28.667	6.527	15.875	41.459	13.000	2.072	8.939	17.061	
Overall	38.713	8.438	22.175	55.251	15.600	2.914	9.888	21.312	

[a]Estimation is limited to the largest survival time if it is censored.

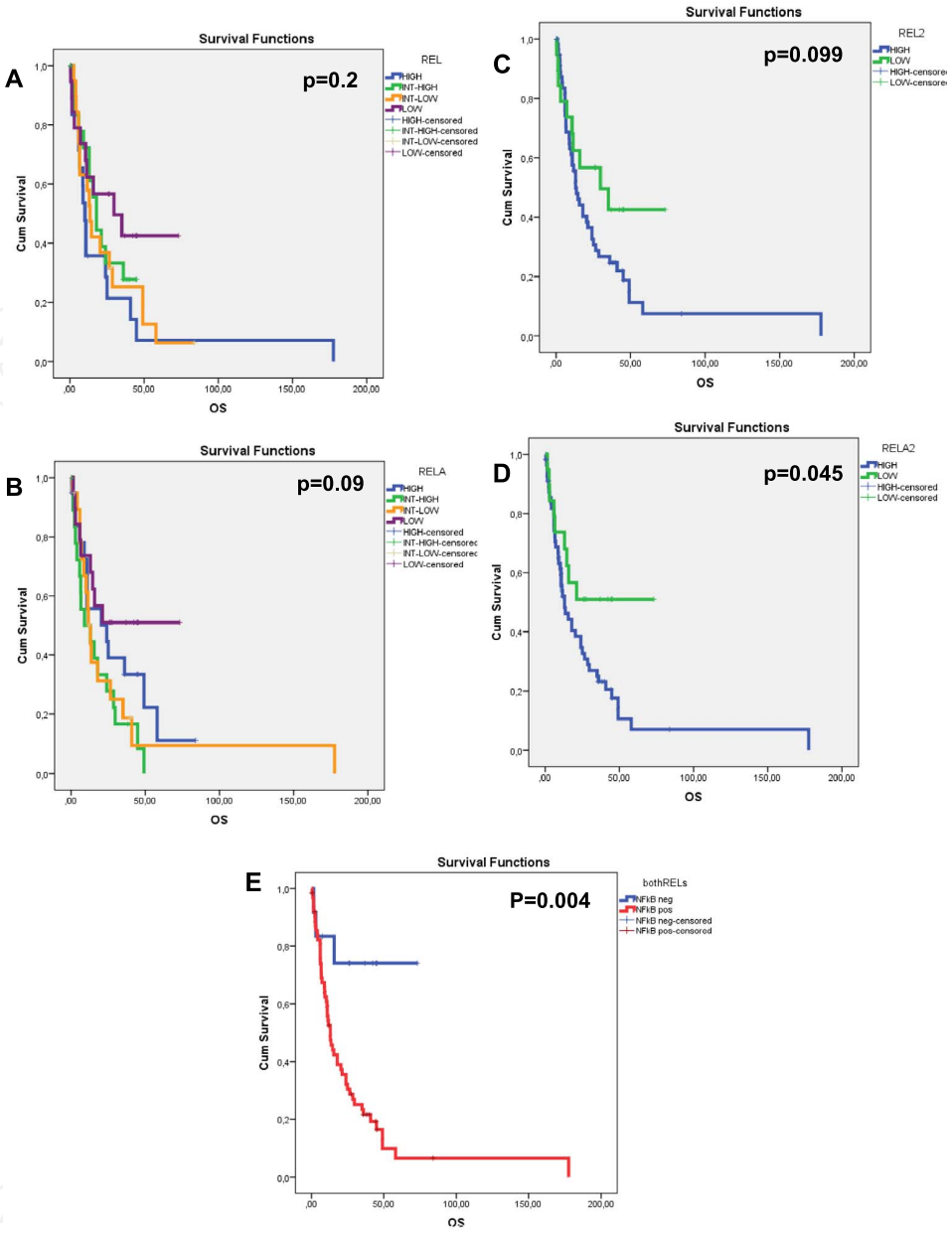

Figure 7. Overall survival (OS) according to NF–kB pathway expression. Kaplan Meier plots for overall survival in PTCL patients according to the expression of REL (A) and RELA (B). Cases were divided into quartiles according to gene expression values (A–B) or into two groups for each molecule, corresponding to Q1 vs. Q2-4 (C–D). Kaplan Meier plots for overall survival in PTCL patients divided into two groups (NF–kB positive vs. NF–kB negative) based on the expression of *REL* and *RELA* (E).

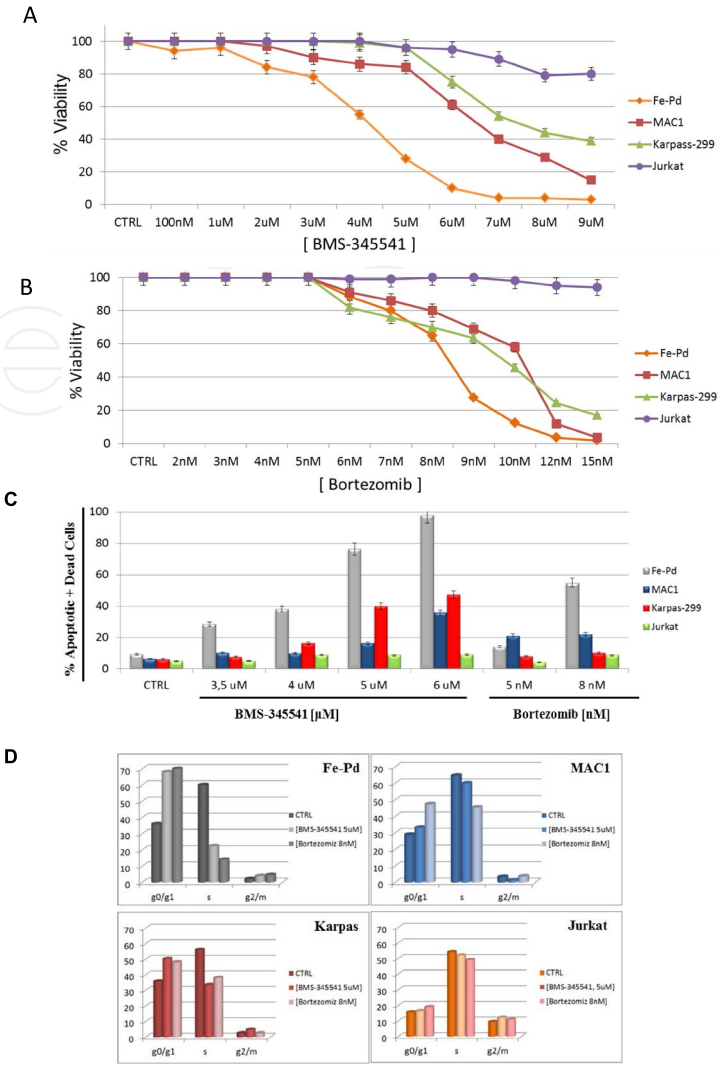

Figure 8. PTCL cells viability upon NF–kB inhibition. The plots graphically show the viability curves for BMS-345541 (A) and Bortezomib (B) after 48 h of incubation in the cell lines. The cell lines growth was inhibited in a dose-dependent manner (CellTiter-Glo Luminescent Cell Viability Assay). The Four cell lines were incubated with increasing concentrations of BMS-345541 and Bortezomib, collected at 48 h and stained with Annexin-V-FITC and propidium iodide (PI) to detect early and late apoptotic cells (A and B, respectively). The histograms show the percentage of apoptotic cells after BMS-345541 and Bortezomib treatment at different concentration (C). Four T-cell lymphoma cell lines were treated with 5 µM (IC_{50}) and 8 nM (IC_{50}) for BMS-345541 and Bortezomib respectively. All cell lines were stained for BrdU and its incorporation detected by flow cytometry (A). Data for progressive cell cycle modification are represented in the histogram as percentage of BrdU positive cells (B). Either BMS-345541 and Bortezomib induced are gradually arrested in G0/G1 phase (D).

Table 4. IC50 values with confidence interval for BMS-345541 after 48 h of incubation (CellTiter-Glo Luminescent Cell Viability Assay).

Cell line	PTCL subtype	BMS-345541 (μM)	BORTEZOMIB (nM)
Fe–Pd	PTCL/NOS CD30+	4,141 (3,8–4,7)	8,35 (8,1–8,6)
MAC1	CTCL	6,59 (6,1–7,1)	10,01 (9,6–10,4)
KARPAS	ALK+_ALCL	6,97 (6,7–7,2)	9,63 (9,0–10,2)
JURKAT	T-ALL	>9	>15

concentrations (3.5–6 μM for BMS-345541; 5–8 nM for Bortezomib). After 48 h, we observed an increase in the apoptotic events up to 76% in Fe–Pd, 36% in MAC1, 47% in Karpas and 9% in Jurkat cells line upon BMS-345541 treatment (figure 8). Similar results we observed when we treated PTCLs cells lines with Bortezomib. Particularly, we documented 58% of apoptotic events in Fe–Pd, 22% in MAC1, 10% in Karpas, and 8% in Jurkat cells lines upon administration of Bortezomib 8 nM. To further assess the specificity of the effects exerted by NF–kB inhibitors on PTCL cells and evaluate the potential toxicity of such treatment, we investigated the induction of apoptosis in PBMCs from healthy donors. Healthy donor PBMCs were exposed to BMS-345541 at 5 μM and Bortezomib at 8 nM (IC50) for 48 h. Importantly, we did not record any significant cytotoxicity or apoptosis induction in non-neoplastic T-cells (supplementary figure 6).

Finally, to prove that the observed pharmacologic effects were associated with NF–kB inhibition, we performed immunocytochemical analysis of RELA and p50 expression in Fe–Pd cell line before and after 6 h of treatment with 5 μM BMS-345541. While untreated Fe–Pd cells showed a marked nucleo-cytoplasmic positivity for both RELA and p50 proteins, after incubation with BMS-345541 a dramatic reduction of the nuclear staining with RELA and p50 was observed, the two molecules expression being substantially confined to the cytoplasm (supplementary figure 7).

Taken together, these data indicate that NF–kB inhibition is effective against NF–kB positive PTCL cells *ex vivo*.

4. Discussion

In this paper we thoroughly explored NF–kB effectors expression in a large series of PTCLs/NOS by gene expression analysis. We documented for the first time a relatively high prevalence of NF–kB activation in PTCL/NOS in comparison with previous reports [6, 7, 13]. However, it should be noted that previous works mainly focused on RELA expression, while our investigation included REL and RELB as well. If we limited the analysis to RELA, our data would perfectly parallel previous observations. Indeed, the present results are also in line with previous evidences of TCR signaling integrity in PTCL/NOS [19], as NF–kB is one of the main downstream TCR targets. Particularly, our data are in line with evidences supporting the activity

of SYK tyrosine kinase in most PTCL/NOS [36]. Interestingly, our data indicated for the first time that different mechanisms might be responsible for NF–kB triggering in PTCL. In fact, *RELA* over-expression was strictly associated to TCR signaling, being related with either TCR structural components (*CD3E*, *CD5*, *CD7*) and TCR costimulatory molecules (*ICOS*, *CTLA4*, and *CD28*) and TCR downstream (*STAT1* and *STAT3*). Conversely, *REL* overexpression was at least partially independent from TCR, not showing such correlations. In line with this, we found that the transcriptional network of *RELA* and *REL*, as inferred by reverse engineering and largely validated by previous biochemical evidence, were only partially, though significantly, overlapping. Genes belonging to both networks are known to be functionally related, as many protein-protein interactions have been described and are involved in mRNA maturation and splicing, lymphocyte differentiation and inflammatory response. Remarkably, they turned out to be significantly enriched in genes regulated by PDGF/PDGFRs axis as well, suggesting the hypothesis that NF–kB pathway and PDGFRA signaling may converge in PTCL cells [8, 9, 37, 38]. On the other hand, RELA, maybe through the intermediate STATs proteins, appeared to have a larger network of neighbors if compared to REL. When analyzed for their involvement in cellular function, RELA neighbors appeared to be significantly related to transcription regulation, intracellular signaling cascade (including tyrosine kinase cascades), and often involved in known oncopathways, such as those mastered by TBK1, E2F1, RB, MTOR and EGFR.

The evidence of TCR/NF–kB activity in these tumors raises the question whether such activation is constitutive rather than mediated by microenvironmental stimuli, as physiologically happens in T-lymphocytes. So far, a few studies investigated the mutational landscape of PTCL/NOS [39, 40] but failed to identify consistent genetic abnormalities potentially responsible for NF–kB constitutive activation. On the other hand, in a SNPs array study, it was shown that REL locus is quite rarely affected by amplifications leading to *REL* up-regulation and activation of the pathway [17]. Therefore, the intriguing hypothesis of a contribution from reactive components has to be certainly explored in future studies. To this regard, trying to dissect the contribution of microenvironment-related and neoplastic cell-intrinsic events to the engagement of such a redundant molecular network in PTCL is a great challenge. Indeed, the reactive milieu of PTCLs is highly variable and dramatically influenced by the neoplastic clone biology [41, 42] and may be differently enriched in inflammatory or regulatory cells such as IL-17-secreting T helper lymphocytes or regulatory T cells. Furthermore, NF–kB pathways may also be sustained by autocrine loops involving the neoplastic clone such as that of PDGFA/PDGFRA axis, which share many cellular effects (e.g. cell proliferation) [4, 43]. Recently, miRNA deregulation, a common feature in PTCL/NOS [44], has been related to NF–kB pathway activation in this setting. In particular, it was found that microRNA-146a

down-regulates NF–kB activity via targeting TRAF6, thus functioning as tumor suppressor element [45].

The robustness of our classification system into NF–kB positive and NF–kB negative cases was validated biologically. We showed that the two groups presented with differential expression of genes known to be transcriptional target of NF–kB, differential enrichment in NF–kB pathway cascade, and TCR-signaling related genes. This translated in the differential expression of genes related to lymphocyte activation, blockage of programmed cell death/apoptosis, and cell proliferation. In this regard, we showed that the molecular profile of PTCL/NOS is closer to that of activated rather than resting T-lymphocytes [9]; which is in line with NF–kB pathway playing a central role in physiological T-cell development and activation. In fact, it has been demonstrated that NF–kB activation by TCR is necessary and sufficient for T-cell activation and survival *in vivo* [46]. As far as NF–kB negative cases were concerned, it should be noted that different studies by our and other groups indicated BCL10 down-regulation in PTCL/NOS, this molecule being an upstream activator of NF–kB [9, 13, 20]. Recent studies, based on next generation sequencing, also showed that somatic mutation can affect NF–kB pathway at different levels [47].

The distinction of PTCLs according to NF–kB status was also validated clinically. In fact, cases classified as NF–kB negative showed a significantly better OS. This finding is in line with previous evidences that tumors provided with higher proliferation rate (documented by either immunohistochemistry or gene expression profiling) have a more aggressive course [13, 33]. By contrast, a couple of studies showed a better outcome for NF–kB cases [7, 13]; however, both these studies were limited to RELA, significantly underestimating the NF–kB positive group. As REL family members mRNA quantization is relatively easy and cheap, if their prognostic role will be confirmed in independent, possibly prospective, studies, it may become a novel biomarker for patients' prognostication in clinic. Conversely, our data are consistent with more recent evidence that expression of NIK, an upstream controller of NF–kB pathways, is associated with a poor outcome in PTCLs [48].

Based on the evidence that the pathway is active in a fraction of cases, this being also related to an adverse outcome with conventional chemotherapy, we tested whether NF–kB inhibition might be a rational therapeutic strategy. A similar approach had been previously adopted for diffuse large B-cell lymphomas (DLBCL); in this setting, in fact, NF–kB activation is related to a worse outcome and can be efficiently targeted in vivo [48–54]. We found that the unique available PTCL/NOS cell line was characterized by NF–kB activation and its inhibition by both a IKKB specific inhibitor or a proteasome inhibitor led to cell cycle blockage and finally cell death. Recent clinical data suggested only a modest activity of bortezomib in PTCL patients [24]. However, no case selection was operated and a possible relation

between efficacy and NF–kB inhibition was assessed by using immunohistochemistry, the interpretation of which in PTCL cases with usually abundant reactive components is subjective and more often indeed problematic. By contrast, in CTCL, that are usually NF–kB positive, bortezomib was quite successful [23].

In conclusion, we performed for the first time, a thorough investigation of NF–kB expression and activation in PTCL/NOS, documenting its negative prognostic role. Further, we provided a biological rationale for adopting NF–kB inhibition strategies in a subset of PTCL/NOS cases. Future studies should confirm the prognostic relevance of NF–kB status in prospective independent series, identify the key events underlying NF–kB activation/shut off in PTCL clones, and explore the clinical efficacy of NF–kB inhibition in PTCL/NOS patients.

Data availability

Gene expression raw data are available at GEO website (https://www.ncbi.nlm.nih.gov/geo/) (see specific datasets in the Material and Methods section).

Conflict of interest

The Authors have no conflict of interest to disclose.

Funding

This work was supported by BolognAIL, Prof. Piccaluga, RFO (Prof. Piccaluga), and FIRB Futura 2011 RBFR12D1CB (Prof. Piccaluga). The authors have no conflicting financial interests to declare.

Authors contribution

PPP coordinated the research and performed molecular analyses. MN, CA and PPP wrote the manuscript. CA, and PW, were responsible for case collection, immunohistochemistry and data analysis. FR, PLT, DG, were involved in case collection, flow cytometry and molecular analyses. The authors reported no potential conflicts of interest.

Supplementary materials

Supplementary materials are available at https://cdn.intechopen.com/journals/docs/Supplementary_Data.zip.

Acknowledgements

The Authors are grateful to Dr. Maria Antonella Laginestra, Dr. Simona Righi, Dr. Maura Rossi, and Dr. Maria Teresa Sista for the skilled technical assistance, and to Dr. Guarguaglini for medicine support.

References

1 **Jaffe E. S.**, **Harris N. L.**, **Stein H. et al.** Introduction and overview of the classification of the lymphoid neoplasms. In: Swerdlow S., Campo E., Harris N. L., Jaffe E. S., Pileri S. A., Stein H. et al. (eds), WHO Classification of Tumors of Hematopoietic and Lymphoid Tissues. IV ed, Lyon: IARC, 2017.

2 **Pileri S.A.**, **Weisenburger D. D.**, **Sng I. et al.** Peripheral T-cell lymphoma, not otherwise specified. In: Swerdlow S., Campo E., Harris N. L., Jaffe E. S., Pileri S. A., Stein H. (eds), WHO Classification of Tumors of Hematopoietic and Lymphoid Tissues. IV ed, Lyon: IARC, 2008; pp. 306–308.

3 **Agostinelli C.**, **Piccaluga P. P.**, **Went P. et al.** Peripheral T cell lymphoma, not otherwise specified: the stuff of genes, dreams and therapies. ***J. Clin. Pathol.***, 2008; **61**(11): 1160–1167.

4 **Pileri S. A.**, **Piccaluga P. P.** New molecular insights into peripheral T cell lymphomas. ***J. Clin. Invest.***, 2012; **122**(10): 3448–3455.

5 **Martinez-Delgado B.**, **Melendez B.**, **Cuadros M. et al.** Expression profiling of T-cell lymphomas differentiates peripheral and lymphoblastic lymphomas and defines survival related genes. ***Clin. Cancer Res.***, 2004; **10**(15): 4971–4982.

6 **Ballester B.**, **Ramuz O.**, **Gisselbrecht C. et al.** Gene expression profiling identifies molecular subgroups among nodal peripheral T-cell lymphomas. ***Oncogene***, 2006; **25**(10): 1560–1570.

7 **Martinez-Delgado B.**, **Cuadros M.**, **Honrado E. et al.** Differential expression of NF-kappaB pathway genes among peripheral T-cell lymphomas. ***Leukemia***, 2005; **19**(12): 2254–2263.

8 **Piccaluga P. P.**, **Agostinelli C.**, **Zinzani P. L. et al.** Expression of platelet-derived growth factor receptor alpha in peripheral T-cell lymphoma not otherwise specified. ***Lancet Oncol.***, 2005; **6**(6): 440.

9 **Piccaluga P. P.**, **Agostinelli C.**, **Califano A. et al.** Gene expression analysis of peripheral T cell lymphoma, unspecified, reveals distinct profiles and new potential therapeutic targets. ***J. Clin. Invest.***, 2007; **117**(3): 823–834.

10 **Piccaluga P.**, **Fuligni F.**, **De Leo A. et al.** Molecular profiling improves classification and prognostication of nodal peripheral T-cell lymphomas. Results of a phase 3 diagnostic accuracy study. ***J. Clin. Oncol.***, 2013; **31**(24): 3019–3025.

11 **Iqbal J.**, **Weisenburger D. D.**, **Greiner T. C. et al.** Molecular signatures to improve diagnosis in peripheral T-cell lymphoma and prognostication in angioimmunoblastic T-cell lymphoma. ***Blood***, 2010; **115**(5): 11.

12 **Iqbal J.**, **Wright G.**, **Wang C. et al.** Gene expression signatures delineate biological and prognostic subgroups in peripheral T-cell lymphoma. ***Blood***, 2014; **123**(19): 2915–2923.

13 **Briones J.**, **Moga E.**, **Espinosa I. et al.** Bcl-10 protein highly correlates with the expression of phosphorylated p65 NF-kappaB in peripheral T-cell lymphomas and is associated with clinical outcome. ***Histopathology***, 2009; **54**(4): 478–485.

14 **Staudt L. M.** Oncogenic activation of NF-kappaB. ***Cold Spring Harb. Perspect. Biol.***, 2010; **2**(6): a000109.

15 **Izban K. F.**, **Pooley R. J.**, **Selvaggi S. M. et al.** Cytologic diagnosis of peripheral T-cell lymphoma manifesting as ascites. ***Case Rep. Acta Cytol.***, 2001; **45**(3): 385–392.

16 **Staal F. J.**, **Langerak A. W.** Signaling pathways involved in the development of T-cell acute lymphoblastic leukemia. ***Haematologica***, 2008; **93**(4): 493–497.

17 **Hartmann S., Gesk S., Scholtysik R. et al.** High resolution SNP array genomic profiling of peripheral T cell lymphomas, not otherwise specified, identifies a subgroup with chromosomal aberrations affecting the REL locus. ***Br. J. Haematol.***, 2010; **148**(3): 402–412.

18 **Hayden M. S., Ghosh S.** Shared principles in NF-kappaB signaling. ***Cell***, 2008; **132**(3): 344–362.

19 **Geissinger E., Sadler P., Roth S. et al.** Disturbed expression of the T-cell receptor/CD3 complex and associated signaling molecules in CD30+ T-cell lymphoproliferations. ***Haematologica***, 2010; **95**(10): 1697–1704.

20 **Rossi M., Agostinelli C., Righi S. et al.** BCL10 down-regulation in peripheral T-cell lymphomas. ***Hum. Pathol.***, 2012; **43**(12): 2266–2273.

21 **Piccaluga P. P., Agostinelli C., Califano A. et al.** Gene expression analysis of angioimmunoblastic lymphoma indicates derivation from T follicular helper cells and vascular endothelial growth factor deregulation. ***Cancer Res.***, 2007; **67**(22): 10703–10710.

22 **Lee J., Suh C., Kang H. J. et al.** Phase I study of proteasome inhibitor bortezomib plus CHOP in patients with advanced, aggressive T-cell or NK/T-cell lymphoma. ***Ann. Oncol.***, 2008; **19**(12): 2079–2083.

23 **Zinzani P. L., Musuraca G., Tani M. et al.** Phase II trial of proteasome inhibitor bortezomib in patients with relapsed or refractory cutaneous T-cell lymphoma. ***J. Clin. Oncol.***, 2007; **25**(27): 4293–4297.

24 **Kim S. J., Yoon D. H., Kang H. J. et al.** Bortezomib in combination with CHOP as first-line treatment for patients with stage III/IV peripheral T-cell lymphomas: a multicentre, single-arm, phase 2 trial. ***Eur. J. Cancer***, 2012; **48**(17): 3223–3231.

25 **Pahl H. L.** Activators and target genes of Rel/NF-kappaB transcription factors. ***Oncogene***, 1999; **18**(49): 6853–6866.

26 **Piccaluga P. P., Califano A., Klein U. et al.** Gene expression analysis provides a potential rationale for revising the histological grading of follicular lymphomas. ***Haematologica***, 2008; **93**(7): 1033–1038.

27 **Piccaluga P. P., De Falco G., Kustagi M. et al.** Gene expression analysis uncovers similarity and differences among Burkitt lymphoma subtypes. ***Blood***, 2011; **117**(13): 3596–3608.

28 **Margolin A. A., Nemenman I., Basso K. et al.** ARACNE: an algorithm for the reconstruction of gene regulatory networks in a mammalian cellular context. ***BMC Bioinform.***, 2006; **7**(Suppl. 1): S7.

29 **Agbottah E., Yeh W. I., Berro R. et al.** Two specific drugs, BMS-345541 and purvalanol A induce apoptosis of HTLV-1 infected cells through inhibition of the NF-kappaB and cell cycle pathways. ***AIDS Res. Ther.***, 2008; **5**: 12.

30 **Marchi E., Paoluzzi L., Scotto L. et al.** Pralatrexate is synergistic with the proteasome inhibitor bortezomib in in vitro and in vivo models of T-cell lymphoid malignancies. ***Clin. Cancer Res.***, 2010; **16**(14): 3648–3658.

31 **Chou T.** Relationships between inhibition constants and fractional inhibition in enzyme-catalyzed reactions with different numbers of reactants, different reaction mechanisms, and different types and mechanisms of inhibition. ***Mol. Pharmacol.***, 1974; **10**(2): 235–247.

32 **Sapienza M. R., Fuligni F., Agostinelli C. et al.** Molecular profiling of blastic plasmacytoid dendritic cell neoplasm reveals a unique pattern and suggests selective sensitivity to NF–kB pathway inhibition. ***Leukemia***, 2014; **28**(8): 1606–1616.

33 **Went P., Agostinelli C., Gallamini A. et al.** Marker expression in peripheral T-cell lymphoma: a proposed clinical-pathologic prognostic score. ***J. Clin. Oncol.***, 2006; **24**(16): 2472–2479.

34 **Lorie I., Glavatskaia Iu A., Ryzhko V. V. et al.** A case of unclassifiable peripheral T-cell lymphoma. ***Ter. Arkh.***, 2002; **74**(7): 65–67.

35 **Bastian L., Hof J., Pfau M. et al.** Synergistic activity of bortezomib and HDACi in preclinical models of B-cell precursor acute lymphoblastic leukemia via modulation of p53, PI3K/AKT, and NF-kappaB. ***Clin. Cancer Res.***, 2013; **19**(6): 1445–1457.

36 **Feldman A. L.**, **Sun D. X.**, **Law M. E. et al.** Overexpression of Syk tyrosine kinase in peripheral T-cell lymphomas. ***Leukemia***, 2008; **22**(6): 1139–1143.

37 **Pileri S. A.**, **Piccaluga PP.** New molecular insights into peripheral T cell lymphomas. ***J. Clin. Invest.***, 2012; **122**(10): 3448–3455.

38 **Piccaluga P. P.**, **Tabanelli V.**, **Pileri S. A.** Molecular genetics of peripheral T-cell lymphomas. ***Int. J. Hematol.***, 2014; **99**(3): 219–226.

39 **Palomero T.**, **Couronne L.**, **Khiabanian H. et al.** Recurrent mutations in epigenetic regulators, RHOA and FYN kinase in peripheral T cell lymphomas. ***Nat. Genet.***, 2014; **46**(2): 166–170.

40 **Schatz J. H.**, **Horwitz S. M.**, **Teruya-Feldstein J. et al.** Targeted mutational profiling of peripheral T-cell lymphoma not otherwise specified highlights new mechanisms in a heterogeneous pathogenesis. ***Leukemia***, 2014; **29**(1): 237–241.

41 **Tripodo C.**, **Gri G.**, **Piccaluga P. P. et al.** Mast cells and Th17 cells contribute to the lymphoma-associated pro-inflammatory microenvironment of angioimmunoblastic T-cell lymphoma. ***Am. J. Pathol.***, 2010; **177**(2): 792–802.

42 **Bruneau J.**, **Canioni D.**, **Renand A. et al.** Regulatory T-cell depletion in angioimmunoblastic T-cell lymphoma. ***Am. J. Pathol.***, 2010; **177**(2): 570–574.

43 **Piccaluga P. P.**, **Rossi M.**, **Agostinelli C. et al.** Platelet-derived growth factor alpha mediates the proliferation of peripheral T-cell lymphoma cells via an autocrine regulatory pathway. ***Leukemia***, 2014; **28**(8): 1687–1697.

44 **Laginestra M. A.**, **Piccaluga P. P.**, **Fuligni F. et al.** Pathogenetic and diagnostic significance of microRNA deregulation in peripheral T-cell lymphoma not otherwise specified. ***Blood Cancer J.***, 2014; **4**(11): 259. doi:10.1038/bcj.2014.78.

45 **Paik J. H.**, **Jang J. Y.**, **Jeon Y. K. et al.** MicroRNA-146a downregulates NFkappaB activity via targeting TRAF6 and functions as a tumor suppressor having strong prognostic implications in NK/T cell lymphoma. ***Clin. Cancer Res.***, 2011; **17**(14): 4761–4771.

46 **Zheng Y.**, **Vig M.**, **Lyons J. et al.** Combined deficiency of p50 and cRel in CD4+ T cells reveals an essential requirement for nuclear factor kappaB in regulating mature T cell survival and in vivo function. ***J. Exp. Med.***, 2003; **197**(7): 861–874.

47 **Schatz J. H.**, **Horwitz S. M.**, **Teruya-Feldstein J. et al.** Targeted mutational profiling of peripheral T-cell lymphoma not otherwise specified highlights new mechanisms in a heterogeneous pathogenesis. ***Leukemia***, 2015; **29**(1): 237–241.

48 **Odqvist L.**, **Sanchez-Beato M.**, **Montes-Moreno S. et al.** NIK controls classical and alternative NF-kappaB activation and is necessary for the survival of human T-cell lymphoma cells. ***Clin. Cancer Res.***, 2013; **19**(9): 2319–2330.

49 **Alizadeh A. A.**, **Eisen M. B.**, **Davis R. E. et al.** Distinct types of diffuse large B-cell lymphoma identified by gene expression profiling. ***Nature***, 2000; **403**(6769): 503–511.

50 **Rosenwald A.**, **Wright G.**, **Chan W. C. et al.** The use of molecular profiling to predict survival after chemotherapy for diffuse large-B-cell lymphoma. ***N. Engl. J. Med.***, 2002; **346**(25): 1937–1947.

51 **Davis R. E.**, **Brown K. D.**, **Siebenlist U. et al.** Constitutive nuclear factor kappaB activity is required for survival of activated B cell-like diffuse large B cell lymphoma cells. ***J. Exp. Med.***, 2001; **194**(12): 1861–1874.

52 **Rabson A. B.**, **Weissmann D.** From microarray to bedside: targeting NF-kappaB for therapy of lymphomas. ***Clin. Cancer Res.***, 2005; **11**(1): 2–6.

53 **Dunleavy K.**, **Pittaluga S.**, **Czuczman M. S. et al.** Differential efficacy of bortezomib plus chemotherapy within molecular subtypes of diffuse large B-cell lymphoma. ***Blood***, 2009; **113**(24): 6069–6076.

54 **Gaurnier-Hausser A.**, **Patel R.**, **Baldwin A. S. et al.** NEMO-binding domain peptide inhibits constitutive NF-kappaB activity and reduces tumor burden in a canine model of relapsed, refractory diffuse large B-cell lymphoma. ***Clin. Cancer Res.***, 2011; **17**(14): 4661–4671.